

# Crystal Structure and Photodynamic Behavior of the Blue Emission Variant Y66H/Y145F of Green Fluorescent Protein<sup>†</sup>

Rebekka M. Wachter,<sup>‡</sup> Brett A. King,<sup>§</sup> Roger Heim,<sup>||</sup> Karen Kallio,<sup>‡</sup> Roger Y. Tsien,<sup>||</sup> Steven G. Boxer,<sup>§</sup> and S. James Remington<sup>\*;‡</sup>

*Institute of Molecular Biology and Department of Physics, University of Oregon, Eugene, Oregon 97403, Department of Pharmacology and Howard Hughes Medical Institute 0647, University of California, San Diego, La Jolla, California 92093, and Department of Chemistry, Stanford University, Stanford, California 94305*

Received March 12, 1997; Revised Manuscript Received June 2, 1997<sup>⊗</sup>

**ABSTRACT:** The crystal structure of a blue emission variant (Y66H/Y145F) of the *Aequorea victoria* green fluorescent protein has been determined by molecular replacement and the model refined. The crystallographic *R*-factor is 18.1% for all data from 20 to 2.1 Å, and the model geometry is excellent. The chromophore is non-native and is autocatalytically generated from the internal tripeptide Ser65-His66-Gly67. The final electron density maps indicate that the formation of the chromophore is complete, including 1,2 dehydration of His66 as indicated by the planarity of the chromophore. The chromophore is in the *cis* conformation, with no evidence for any substantial fraction of the *trans* configuration or uncyclized apoprotein, and is well-shielded from bulk solvent by the folded protein. These characteristics indicate that the machinery for production of the chromophore from a buried tripeptide unit is not only intact but also highly efficient in spite of a major change in chromophore chemical structure. Nevertheless, there are significant rearrangements in the hydrogen bond configuration around the chromophore as compared to wild-type, indicating flexibility of the active site. pH titration of the intact protein and the chromopeptide ( $pK_{a1} = 4.9 \pm 0.1$ ,  $pK_{a2} = 12.0 \pm 0.1$ ) suggests that the predominant form of the chromophore in the intact protein is electrically neutral. In contrast to the wild-type protein [Chattoraj, M., King, B. A., Bublitz, G. U., & Boxer, S. G. (1996) *Proc. Natl. Acad. Sci. U.S.A.*, 8362–8367], femtosecond fluorescence up-conversion spectroscopy of the intact protein and a partially deuterated form strongly suggests that excited-state proton transfer is not coupled to fluorescence emission.

The green fluorescent protein (GFP)<sup>1</sup> from the jellyfish *Aequorea victoria* is an exceptionally versatile and useful tool for biotechnological applications. A number of recent reviews have described its uses and expression in a variety of organisms (Cubitt et al., 1995; Prasher, 1995; Gerdes & Kaether, 1996). The protein owes its utility to the spontaneous formation of the fluorophore from the internal cyclization and 1,2 dehydration of the central residue in the internal peptide -Ser65-Tyr66-Gly67-. The only external factor required for the appearance of visible fluorescence is molecular oxygen. The usefulness of the protein as a fluorescent label is enhanced by the availability of mutants with a broad range of absorption and emission maxima (Heim et al., 1994; Ormö et al., 1996), permitting both multicolor reporting of cellular processes (Rizzuto et al., 1996) and resonance energy transfer measurements between GFP molecules with appropriately overlapping emission and absorption spectra and close spatial proximity (Heim & Tsien, 1996; Mitra et al., 1996).

Recently, femtosecond fluorescence up-conversion spectroscopy has demonstrated rich photodynamic behavior in wild-type GFP (WT).<sup>1</sup> WT has absorption maxima at about 395 and 475 nm. Irradiation at 395 nm results in a time-delayed emission at 508 nm that is slowed dramatically upon exchanging protons with deuterons, indicating proton transfer in the excited state (Chattoraj et al., 1996). In contrast, irradiation at 475 nm results in an essentially instantaneous onset of fluorescence. Upon continued irradiation at 395 nm, the absorption at 395 nm is slowly reduced with concomitant increase in the 475 nm absorption that is reversible upon dark-adaptation. A detailed atomic model, based on a comparison of the crystal structures of wild-type (Brejc et al., 1997) and S65T (Ormö et al., 1996) for proton motion between the chromophore and a hydrogen bond network of neighboring side chains accounting for this behavior has been proposed.

The GFP variant P4-3 (blue fluorescent protein, or BFP; Heim et al., 1994)<sup>1</sup> with the substitutions Y66H/Y145F has been described previously (Heim & Tsien, 1996). This mutant also contains the innocuous Q80R mutation that was evidently accidentally introduced early in the cloning of the cDNA (Chalfie et al., 1994). The absorption and emission maxima (382 and 448 nm, respectively; Heim et al., 1994) are radically altered from wild-type by substitution of His for Tyr in the tripeptide that becomes the fluorophore upon autocatalytic cyclization/oxidation. Resonance energy transfer between BFP and the S65T variant has been demonstrated (Heim & Tsien, 1996; Mitra et al., 1996), suggesting that this pair of proteins can be used as a reporter of the spatial proximity of two appropriately labeled protein molecules or

<sup>†</sup> This work was supported in part by grants from the Office of Naval Research (Contract N00014-91-C-0170), the National Institutes of Health, and the National Science Foundation (Grant MCB 9418479 to S.J.R.).

\* To whom correspondence should be addressed.

<sup>‡</sup> University of Oregon.

<sup>§</sup> Stanford University.

<sup>||</sup> Howard Hughes Medical Institute and University of California, San Diego.

<sup>⊗</sup> Abstract published in *Advance ACS Abstracts*, August 1, 1997.

<sup>1</sup> Abbreviations: BFP, GFP variant P4-3 (GFP Y66H/Y145F) or blue fluorescent protein; WT, wild-type GFP; BFP-D, partially deuterated BFP; OD, optical density.

other cellular processes. In order to investigate the efficiency of formation of the chromophore, its conformation and three-dimensional environment, we determined the crystal structure of BFP by molecular replacement using the previously determined structure of the S65T variant (Ormö et al., 1996). In order to study excited state proton motion, we investigated the photodynamic behavior of the protein in H<sub>2</sub>O and D<sub>2</sub>O by femtosecond fluorescence up-conversion spectroscopy, and have also titrated the intact protein and the chromopeptide obtained by limit digest of BFP with papain. The combined results give a consistent picture of the environment and charge species of both the ground and UV excited states of the blue fluorophore.

## MATERIALS AND METHODS

**Protein Expression and Crystallization.** Histidine-tagged BFP was overexpressed in the plasmid JM109/pRSET<sub>B</sub>, and growth and purification were carried out as described for the S65T variant (Ormö et al., 1996). For crystallization, the His-tag was removed by chymotryptic digestion as described (Ormö et al., 1996). The correct NH<sub>2</sub>-terminus was verified by amino acid sequencing, and protein purity was checked by reverse-phase HPLC and SDS-PAGE. BFP was then concentrated to approximately 12 mg/mL in 10 mM HEPES, pH 7.0. Rod-shaped crystals were obtained at 4 °C in hanging drops containing 2  $\mu$ L of protein and 2  $\mu$ L of well solution within 2–6 days. The well solution contained 100 mM sodium acetate, pH 4.5 or 4.6, and 10–12% polyethylene glycol (PEG 3400, Polysciences). Crystals were 0.06–0.1 mm across and up to 0.6 mm long.

**Diffraction Data Collection and Structure Refinement.** X-ray diffraction data were collected from a single crystal at room temperature using a Xuong–Hamlin area detector (Hamlin, 1985). Data were collected to 87% completeness at 2.1 Å resolution, and reduced using the supplied software (Howard et al., 1985). The GFP S65T coordinate file (Ormö et al., 1996) which served as a model for phasing was edited to reflect the mutations. Rigid body refinement was sufficient to determine the orientation of the model in the BFP unit cell, using the program TNT (Tronrud et al., 1987); then initial positional refinement was carried out using the data to 2.8 Å resolution. Electron density maps ( $2F_o - F_c$  and  $F_o - F_c$ ) were inspected, and the model was adjusted using FRODO (Jones, 1982) and O (Jones et al., 1991) with additional positional refinement, using all of the data to the limiting resolution. Solvent molecules were added to the model where appropriate as judged from  $F_o - F_c$  maps and proximity of hydrogen bond partners.

**pH Titrations.** Samples of BFP, both with the His-tag removed and with the His-tag intact, were concentrated to 10 mg/mL in a final volume of approximately 2 mL, and buffer-exchanged into 10 mM HEPES, pH 7.0. Aliquots were stored at 4 °C. A series of buffers at 100 mM concentration were prepared between pH 2 and 10, using phosphate (pH 2.0), formate (pH 3.0–4.2), citrate (pH 4.4–5.8), PIPES (pH 6.0–6.5), HEPES (pH 7.0), Tris (pH 8.0), CHES (pH 9.0), and CAPS (pH 10). The buffer pH was adjusted with a Phi 31 pH meter (Beckman). Buffers at pH 11 and 12 were prepared using standardized pH capsules (Hydriion) since glass electrodes cannot provide accurate measurements at this high pH. Stock solutions at yet higher pH (12.2–14) were prepared by dilution of 1 M NaOH into water. The NaOH concentration in these solutions was

between 1 M and 10 mM, significantly higher than the concentration of BFP, which was 40  $\mu$ M after dilution with buffer.

For each absorbance scan, an aliquot of concentrated BFP was diluted 10-fold with the appropriate buffer and filtered through a 0.22  $\mu$ m filter. Spectrophotometric assays were started 1–2 min after dilution to minimize potential chromophore degradation which was found to be significant at pH 13 and 14, and below pH 3. The absorbance of the sample was scanned at room temperature between 500 and 250 nm against an appropriate buffer blank on a Shimadzu 2101 spectrophotometer.

A papain digest of BFP was prepared essentially according to published procedures (Cody et al., 1993). An aliquot of BFP with the His-tag intact was concentrated to 10 mg/mL in 10 mM HEPES, pH 7.0, thermally denatured at 100 °C for 5 min, and cooled to 37 °C, and papain was added to 10 or 15% by weight. The digest was incubated at 37 °C for a total of 24 h, with reheating to 100 °C and addition of another aliquot of papain after the first 3 h. The disappearance of full-length protein was monitored by reverse-phase HPLC. The major chromopeptide constituted 60% of the 355 nm absorption. Aliquots were frozen immediately at –20 °C, and spectra were later collected after 10-fold dilution into various buffers as described above. The samples were assayed 1–2 min after dilution to minimize chromophore degradation at low or high pH.

The titration curve in Figure 4B was generated by plotting the OD at the absorbance maximum of one of the two charge forms vs pH. This approach proved impractical for the low-pH titration of digested BFP since the absorbance scans were noisy and somewhat variable. The titration curve in Figure 3B was therefore generated by plotting  $A_{370}/A_{340}$  vs pH, where 340 nm is the estimated position of the isosbestic point. This approach results in normalization with respect to protein concentration (Gryniewicz et al., 1985). The  $pK_a$ s of the chromophore in digested BFP were then determined by curve-fitting of the titration data using Kaleidagraph (Synergy Software).  $pK_{a(1)}$  (Figure 3B) is an apparent  $pK_a$  since the position of the isosbestic point is not known precisely.

Fluorescence measurements of BFP samples in their respective buffers were carried out on a Hitachi F4500 fluorescence spectrophotometer at a protein concentration of 0.33 mg/mL. The excitation wavelength was set to the absorbance maximum of the particular sample, and the emission intensity was scanned from 400 to 600 nm at a speed of 2400 nm/min and a slit width for both excitation and emission of 2.5 nm.

**Fluorescence Up-Conversion Spectroscopy.** BFP samples were in 50% glycerol/50% water (v/v) at pH 7.5. Exchangeable protons were replaced by deuterium by diluting the protein with buffer in D<sub>2</sub>O at pH 7.5 (pH meter uncorrected for the isotope effect), and then concentrating the sample to minimum volume, repeated 4 times. The resulting partially deuterated protein is denoted BFP-D and was diluted with glycerol whose hydroxyl protons had been exchanged with deuterium. BFP samples were in this medium 48 h before data were collected.

The time evolution of fluorescence up to 80 ps was measured by fluorescence up-conversion as described by Stanley and Boxer (1995). The samples were excited with the second harmonic of an argon-ion-pumped titanium:sapphire laser. The laser fundamental had a pulse duration of 120 fs and a spectral bandwidth of 111  $\text{cm}^{-1}$  which

Table 1: Data Collection and Atomic Model Statistics of GFP Y66H/Y145F (BFP)

total observations	31786
unique reflections	12044
completeness <sup>a</sup> (%)	87
completeness (shell <sup>b</sup> ) (%)	65
$R_{\text{merge}}^c$ (%)	4.1
resolution (Å)	2.1
atomic model statistics	
crystallographic $R$ -factor	0.181
protein atoms	1784
solvent atoms	81
bond length deviations (Å)	0.010
bond angle deviations (deg)	2.0
thermal parameter restraints (Å <sup>2</sup> )	5.2

<sup>a</sup> Completeness is the ratio of the number of observed  $I > 0$  divided by the theoretically possible number of intensities. <sup>b</sup> Shell is the highest resolution shell (between 2.26 and 2.10 Å). <sup>c</sup>  $R_{\text{merge}} = \sum |I_{hkl} - \langle I \rangle| / \sum \langle I \rangle$  where  $\langle I \rangle$  = average of individual measurements of  $I_{hkl}$ .

corresponds to a time–bandwidth product 35% greater than the theoretical Fourier limit; the second harmonic had a spectral bandwidth of 198 cm<sup>-1</sup>. The cross-correlation of the frequency-doubled output scattering off the sample and the first harmonic used for fluorescence mixing was used as the instrument response function. Its full-width-at-half-maximum was typically 200 fs. Five milliwatts of light was used to excite the sample at 82 MHz. The excitation light was polarized at the magic angle with respect to the detection axis so that the data were not affected by molecular rotation. The samples were stirred in a 1-mm path length quartz cuvette. The cuvette was translated between each scan (i.e., every 1–2 min). The data sets were analyzed by convoluting the instrument response function with a model function composed of at most two exponentials, a base line and a time offset. The parameters of the model function were fit to the collected data by minimizing  $\chi^2$ , which was typically less than 1.2.

## RESULTS AND DISCUSSION

**Crystallographic Analysis.** BFP crystallized in space group  $P2_12_12_1$  isomorphously to wild-type (Brejc et al., 1997), though not under the conditions required for the S65T variant (Ormö et al., 1996); in both cases, there is a monomer in the asymmetric unit. In the S65T crystals, the molecule is displaced by 1.3 Å and reoriented by 1.4° with respect to wild-type, which may be due to the significantly higher pH of crystallization. The C<sub>α</sub> positions of the three models superimpose to approximately 0.5 Å rms. Other crystal forms of GFP whose structures have been solved contain a dimer in the asymmetric unit (Yang et al., 1996), but the significance of dimerization is unclear.

Data collection and atomic model statistics are shown in Table 1. The last nine residues at the C-terminus (residues 230–238) and the surface loop consisting of residues 157 and 158 were found to be disordered and were not modeled. Some disordered side chains with poor electron density were found at the protein surface, and were also not modeled. The final  $R$ -factor of the model was 18.1% for all data between 20 and 2.1 Å resolution, and the rms discrepancies from ideal bond lengths and bond angles were 0.01 Å and 2°, respectively. The final coordinates have been deposited in the Protein Data Bank and have been assigned access code 1BFP.

The chromophore of BFP, though non-native due to the substitution of Tyr66 by histidine, is completely formed, and

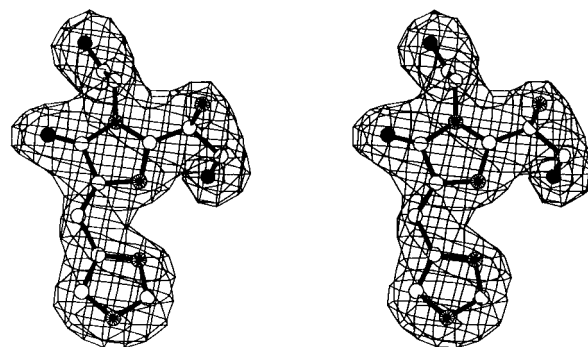


FIGURE 1:  $F_o - F_c$  omit map (occupancy of all chromophore atoms in the model set to zero) at 2.1 Å resolution of the BFP chromophore after refinement. The map is contoured at +3 standard deviations. Oxygen atoms are shown as filled circles, nitrogens as spoked, and carbons as open circles.

is planar (Figure 1). There are no significant features in the final  $F_o - F_c$  difference electron density map near the chromophore, suggesting that there is no significant population of the apoprotein or incompletely oxidized chromophore in the crystals. [The apparent incomplete formation of the chromophore reported for the S65T structure (Ormö et al., 1996) has been subsequently found to be a consequence of the selenomethionine substitution used for phase calculation, and is not seen in the non-selenomethionine substituted crystals (Mats Ormö and S.J.R., unpublished observations).] The chromophore is found to be in the *cis* configuration, as in wild-type. In both structures, *cis*–*trans* isomerization appears to be prevented by the protein scaffold around the chromophore. The two chemical steps responsible for chromophore formation in wild-type GFP, autocatalytic cyclization of Ser65, Tyr66, and Gly67, and  $\alpha,\beta$ -oxidation of Tyr66 in the presence of atmospheric oxygen (Heim et al., 1994), are thus fully functional when the Tyr66 is substituted with histidine.

**Structural Environment of the BFP Chromophore and Proposed Identification of the Charge State.** Comparison of the chromophore environment of BFP with those of wild-type GFP (Brejc et al., 1997) and S65T GFP (Ormö et al., 1996) reveals significant changes in the protein structure adjacent to the chromophore (Figure 2). As compared to S65T, His148 has adjusted to the less bulky chromophore by main chain movement toward the chromophore, and by a 60° flip of the imidazole ring. N<sup>δ</sup> of His148 is hydrogen-bonded to the backbone carbonyl of Arg146 and so must be protonated. After this paper was submitted, the pH 8.5 structure of a BFP containing two other mutations has appeared (Palm et al., 1997), and in this structure, His148 is in an alternative configuration, partially exposed to solvent, not in direct contact with the chromophore, and presumably neutral. Therefore, it is possible that in the present pH 4.5 structure His148 is positively charged (see discussion below).

The carbonyl group derived from the His66 carbonyl is hydrogen-bonded to Arg96, as has been observed for the Tyr66 carbonyl in both the wild-type and S65T structures; however, as in the wild-type structure, Arg96 moves away from the chromophore relative to its position in S65T (where the chromophore is negatively charged), consistent with both wild-type and BFP chromophores being (predominantly) neutral (Brejc et al., 1997). The position of the imidazolone ring formed by backbone cyclization has not changed as compared to wild-type, suggesting that the mechanism of cyclization is not perturbed to any extent by the Y66H

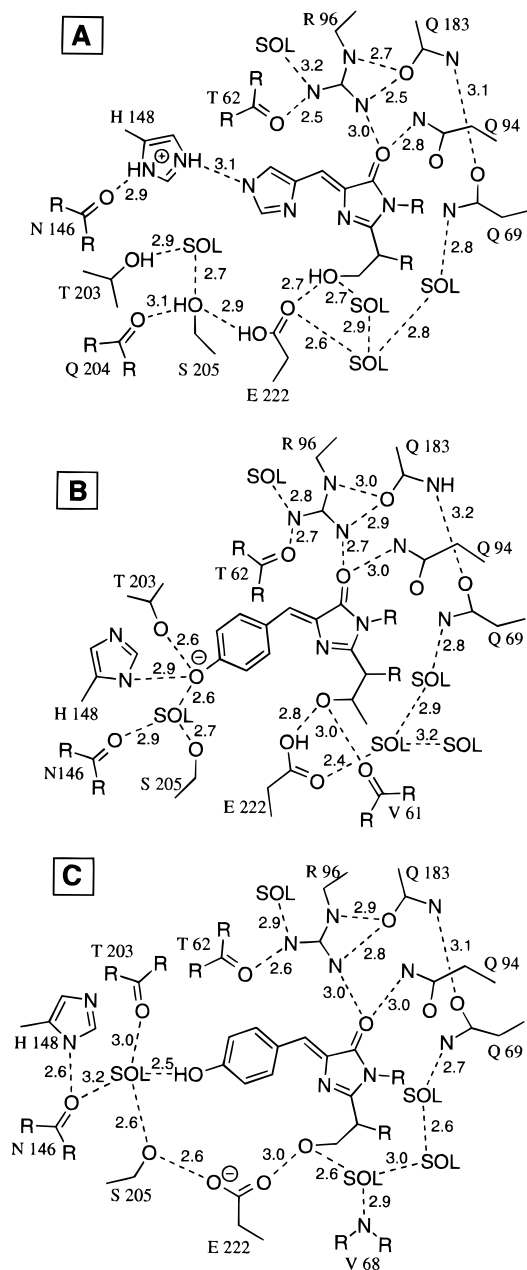
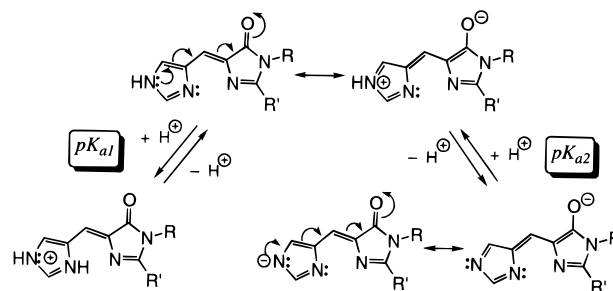


FIGURE 2: Schematic diagram showing the immediate chromophore environment of GFP variants. Panel A: BFP; proposed positions of hydrogens are shown. As discussed in the text, His148 may be positively charged as shown. Panel B: GFP (S65T). Panel C: wild-type GFP.

mutation. Likewise, the remainder of the hydrogen bonding pattern is essentially that of wild-type (Figure 2), except that the water molecule hydrogen-bonded to Ser205 cannot make an analogous hydrogen bond to the BFP chromophore.

For the wild-type protein, a proton relay network has been shown to exist between the phenol hydroxyl, a water molecule, Ser205, and Glu222 which permits rapid proton transfer, and thus charge transfer between the chromophore and Glu222 (Brecj et al., 1997). This network is disrupted between Ser205 and Glu222 in the S65T structure, where Glu222 is inferred to be permanently protonated and the chromophore phenol permanently deprotonated. The BFP structure shows that this network does exist in a manner similar to the wild-type. However, since the water molecule in the network is not hydrogen-bonded to the chromophore, a proton relay between the chromophore and Glu222 is not possible in BFP. Glu222 in the BFP is inferred to be

Scheme 1: Charge States and Resonance Forms of the BFP Chromophore



protonated (Figure 2A) as it is very likely to be a hydrogen bond donor to Ser205.

**pH Titrations of BFP Chromopeptides.** The  $pK_a$ s of the chromophore in solution were investigated in order to explore the possibility that a cationic or anionic chromophore in the protein interior is energetically feasible. In aqueous solution, cationic, neutral, and anionic forms of the chromophore should exist within a pH range that is easily titratable, since the existence of multiple resonance forms should permit lower  $pK_a$ s than those of a simple imidazole ring (Scheme 1). A red-shift in absorbance is expected when deprotonating the cationic species due to more extended  $\pi$ -overlap in the neutral form, and yet a further red-shift is expected when deprotonating the neutral form to give the chromophore anion, principally due to delocalization of the negative charge.

Digestion of BFP by papain yielded a collection of peptides that contained the chromophore, and without further purification, absorbance spectra of the digest were obtained between pH 2 and 14. Three charge states of the chromophore were observed (Scheme 1). Though the low-pH data are noisy, without a clear isosbestic point (Figure 3A), the peptides titrate at  $pH\ 4.9 \pm 0.1$  (Figure 3B). The absorbance maximum of the chromophore shifts from 351 nm at pH 3 to 367 nm at pH 6, and the extinction coefficient approximately doubles. The effect is reversible upon acidification of the pH 6 sample. Between pH 6 and pH 11, the absorbance maximum remains at 367 nm, and is indicative of peptides containing the neutral chromophore. Between pH 11 and 13, the chromophore titrates with a clean isosbestic point at 385 nm (Figure 4A), with the  $\lambda_{max}$  shifting from 367 to 410 nm, indicative of deprotonation to the anionic species.  $pK_{a(2)}$  of the chromophore is revealed to be  $12.0 \pm 0.1$  (Figure 4 B). The shift is also associated with a significant increase in the extinction coefficient.

Since  $pK_{a(1)}$  of imidazole in solution is 7.0 (Albert, 1968), the extended  $\pi$ -electron delocalization over the imidazolinone ring of the chromophore (Scheme 1) leads to a  $pK_a$  drop of approximately 2.1  $pK_a$  units.  $pK_{a(2)}$  is decreased by 2.2  $pK_a$  units as compared to imidazole which has a  $pK_{a(2)}$  of 14.2 (Albert, 1968). The observed decrease of both  $pK_{a(1)}$  and  $pK_{a(2)}$  when comparing imidazole charge states with those of the chromophore formed from cyclization and oxidation of the Ser-His-Gly sequence is entirely consistent with what is known about the wild-type chromophore. The  $pK_a$  of a simple phenol is 9.9 (Weast, 1974), whereas the  $pK_a$  of the *p*-hydroxybenzylideneimidazolinone chromophore has been shown to be 8.1 in unfolded wild-type GFP (Ward, 1980).

**pH Titrations of Intact BFP.** Intact BFP was titrated to investigate the pH dependence of unfolding, and to determine whether the chromophore in the folded protein is in contact

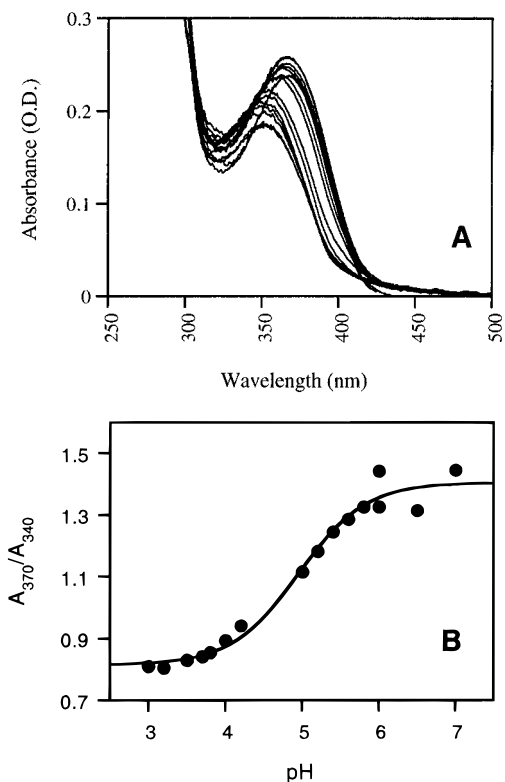


FIGURE 3: pH titration of BFP chromopeptides (acidic range). Panel A: Absorbance scans of the BFP limit digest in various buffers between pH 3.0 and 7.0. Panel B: Apparent titration curve generated from absorbance scans shown in panel A. The absorbance at 370 nm is normalized by taking the ratio  $A_{370}/A_{340}$  for each scan, where 340 nm is the estimated position of the isosbestic point.

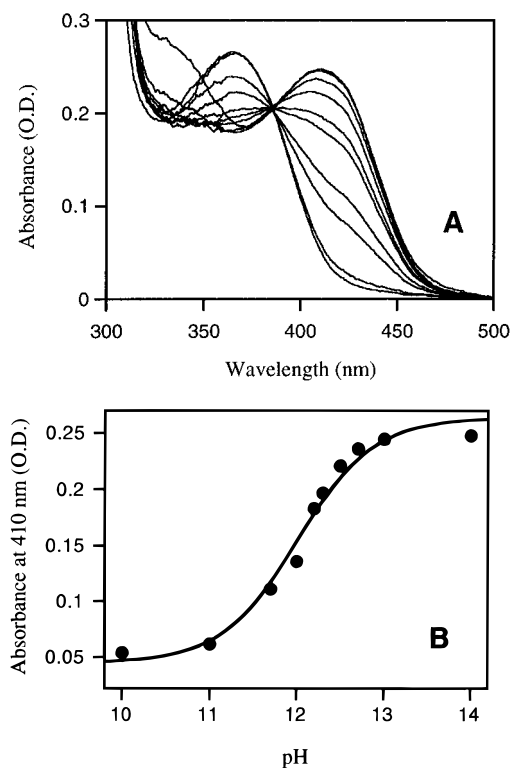


FIGURE 4: pH titration of BFP chromopeptides (basic range). Panel A: Absorbance scans of BFP peptides in various buffers between pH 10 and 14. pH from top to bottom curve (reading at 420 nm): 14, 13, 12.7, 12.5, 12.3, 12.2, 12, 11.7, 11, 10. The curves at pH 10 and 11, and the curves at pH 13 and 14, overlay almost entirely. Panel B: Titration curve generated from data in panel A.

with bulk solvent via a proton relay system. Wild-type GFP is stably folded between pH 4 and 12 (Ward & Bokman,

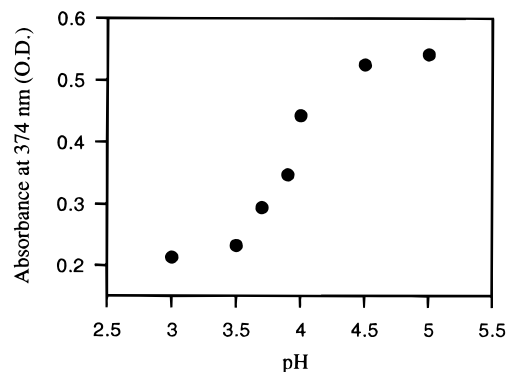


FIGURE 5: Titration curve generated from absorbance scans of intact BFP as a function of pH (pH 3 to pH 5).

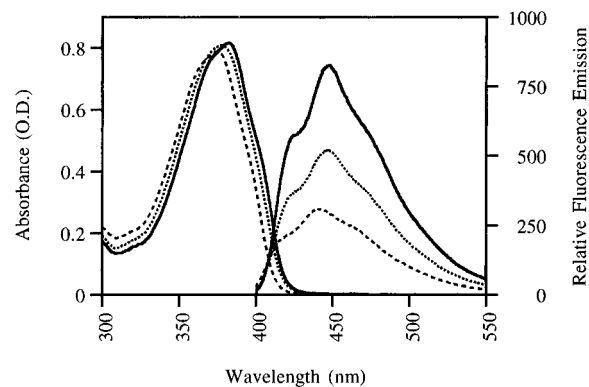


FIGURE 6: Absorbance and relative fluorescence emission of intact BFP. Dashed line, pH 5.0; dotted line, pH 6.0; solid line, pH 7.0. The protein concentration was kept constant for all absorbance scans, and also for all emission scans.

1982), and the protonation state of the chromophore has been shown to be independent of external pH conditions within this range. BFP has been shown to be highly fluorescent within the entire pH range where the protein is stably folded (Cubitt et al., 1995).

The excitation spectrum of the BFP chromophore in the folded protein exhibits an absorbance maximum at 382 nm (Heim et al., 1994; Heim & Tsien, 1996). Absorbance spectra of BFP were obtained in buffer solutions between pH 3 and 14. All scans were initiated 1–2 min after dilution into the appropriate buffer, since chromophore degradation appeared to be a problem upon prolonged incubation, especially above pH 12. A clear isosbestic point at 344 nm was observed when titrating between pH 3 and 5 (data not shown), setting the midpoint for (irreversible) unfolding at pH 3.9 (Figure 5). The absorbance maximum of folded BFP at pH 5.0, 374 nm, is shifted to a maximum of 352 nm in the unfolded state at pH 3.0. Since peptides containing the neutral chromophore absorb at 367 nm and peptides containing the cationic species absorb at 351 nm, it was concluded that the chromophore is neutral in the folded state (folding leads to a red-shift, see below) and cationic in the unfolded state below pH 4.

Between pH 5 and 12, the absorbance spectrum is essentially identical; however, there is a small shift in maximum from 374 to 382 nm between pH 5 and 7 (Figure 6). The fluorescence emission spectra exhibit a similar shift, from 437 nm at pH 5.0 to 446 nm at pH 7.0, concomitant with a significant increase in the quantum yield of fluorescence (Figure 6). The origin of these reversible changes may be due to titration of His148 which contacts the chromophore at low pH, but not at high pH (Palm et al., 1997), and by

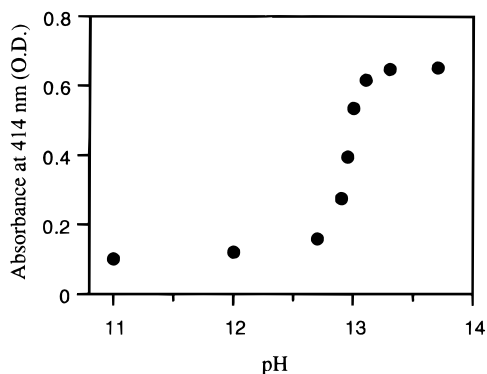


FIGURE 7: Titration curve generated from absorbance scans of intact BFP as a function of pH (pH 11 to pH 13.7).

Table 2: Summary of Absorbance Band Shifts upon GFP Unfolding<sup>a</sup>

	BFP chromophore, neutral	WT chromophore, neutral	WT chromophore, anionic
$\lambda_{\text{ex}}$ folded (nm)	382	395	475
$\lambda_{\text{ex}}$ unfolded or digested (nm)	367	384	448
$\Delta$ (nm)	15	11	27

<sup>a</sup> The data for wild-type GFP were taken from Ward et al. (1980).

virtue of its positive charge alters the electron density distribution of the chromophore. This small shift may be sufficient to allow BFP to be used as a reporter of the pH within cellular compartments.

Titration between pH 11 and 14 gives a second clear isosbestic point at 386 nm (data not shown), indicating conversion of the  $\lambda_{\text{max}}$  of 382 nm in the folded state to the  $\lambda_{\text{max}}$  of 414 nm in the unfolded state at high pH with anionic chromophore (Figure 7). The unfolding transition at high pH exhibits a very steep transition, with the midpoint located at pH 13.0 (Figure 7). The shape of the titration curve may indicate that the  $pK_{a(2)}$  of the chromophore is significantly different in the folded protein as compared to the solution  $pK_a$ , though we have not analyzed the transition in terms of a thermodynamic model since it is irreversible under these experimental conditions. Control experiments with the His-tag intact over the entire pH range from 3 to 14 provided essentially identical results (data not shown).

*The Protein Fold Effects a Red-Shift in Absorbance.* When the BFP chromophore is removed from bulk solvent by the surrounding protein matrix in the folded protein, a red-shift in absorbance of 15 nm is observed (Table 2). A similar red-shift has been observed for both the *Aequorea* and the *Renilla* GFPs. These proteins have identical chromophores formed by cyclization of Ser65, Tyr66, and Gly67, yet the absorbance maxima in the native state of the protein are 393 and 473 nm for *Aequorea*, and 470 and 498 nm for *Renilla* GFP (Ward et al., 1980). When the proteins are unfolded in 6 M guanidine-hydrochloride and heat, both *Aequorea* and *Renilla* GFP absorb at 384 nm at low pH, and at 448 nm at high pH (Table 2). These results are interesting in light of a recent report on solvent polarity studies on a model compound of the wild-type GFP chromophore produced by synthetic means, where it was shown that the absorption spectra shifted to shorter wavelength with increasing solvent polarity (Niwa et al., 1996). The authors suggest that the microenvironment of the chromophore in GFP is similar to 2-propanol in overall polarity.

Table 3: Lifetimes and Amplitudes for the Decay Components of the Excited State of BFP and BFP-D at Room Temperature<sup>a</sup>

	amplitude (%)	$\tau$ (ps)
BFP	$15.50 \pm 3.75$	$2.70 \pm 1.20$
(with His-tag)	$84.50 \pm 3.75$	undetermined
BFP-D	$15.60 \pm 5.83$	$3.20 \pm 1.62$
(with His-tag)	$84.40 \pm 5.83$	undetermined
BFP	$18.53 \pm 2.30$	$2.797 \pm 1.010$
(processed)	$81.47 \pm 2.30$	undetermined
BFP-D	$17.44 \pm 3.26$	$2.997 \pm 1.466$
(processed)	$52.56 \pm 3.26$	undetermined

<sup>a</sup> All samples were excited at 389 nm, and emission was monitored at 450 nm. In processed BFP, the His-tag has been cleaved off by proteolytic digestion.

*The Transfer of a Proton Is Not Coupled to Excited State Decay.* Evidence from titration data suggested that the chromophore in folded BFP is in the neutral state. The anionic form of the chromophore would be interesting from the point of view of practical applications, as it exhibits both an increased extinction coefficient and a considerable red shift (Figure 4A). Rapid temporary proton transfer from the neutral chromophore to nearby acceptors could occur (Figure 2). However, it is unlikely that the anionic form exists in equilibrium with the neutral form in the ground state of the chromophore as this should lead to two well-separated absorbance maxima and this is not observed. On the other hand, if the  $pK_a$  of the chromophore drops sufficiently upon excitation, as has been shown to be true for wild-type GFP (Chattoraj et al., 1996), proton transfer to His148 or another acceptor might be observed. For this reason, we investigated the excited state dynamics of BFP.

To determine whether or not BFP undergoes excited state proton transfer, we measured the early time emission from both BFP and BFP-D at room temperature following excitation of the single absorption band peaked at 383 nm. Excitation at 389 nm leads to an instantaneous (within the instrument response) appearance of fluorescence at 450 nm that persists out to 80 ps (the longest time observed), with a small decay over this time scale. Deuteration does not have a significant effect on the excited state dynamics (Table 3 and Figure 8); the fast component slows by 20% in BFP-D, but this is within the error of the measurement. As we observe only the first 80 ps of the emission, the long time decay component is ill-determined [i.e., the lifetime of this component is significantly longer than 80 ps, which is consistent with the reported lifetime of 0.9 ns (Lossau et al., 1996)] but appears to be similar for both samples. The same experiment was done on poly-His-tagged BFP and BFP-D to determine whether the tag affected the excited state dynamics or was responsible for any feature in the kinetics; the kinetics are similar for the tagged and untagged proteins (Table 3). In conclusion, proton transfer is not coupled to fluorescence emission from the excited state of BFP, in keeping with the absorption spectrum which shows only a single absorption band.

## CONCLUSIONS

Given the desirability of engineering fluorescent proteins with differing absorption and emission characteristics and the unusual nature of the autocatalytic formation of the chromophore in GFP, it seemed important to systematically investigate the properties of the available variants that have been discovered by random mutagenesis. We chose to

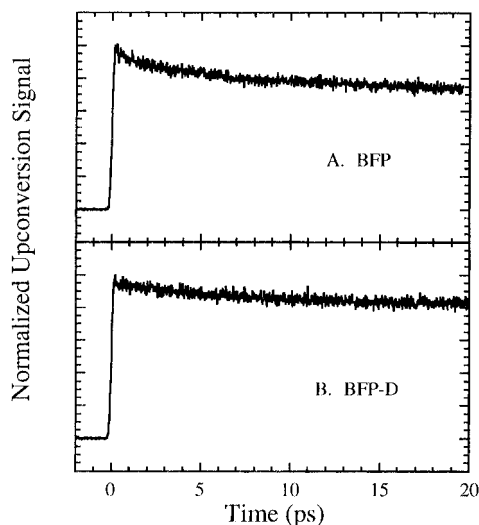


FIGURE 8: Room temperature time-resolved fluorescence of BFP (A) and BFP-D (B) excited at 389 nm and detected at 450 nm. The number of counts at the maximum of each decay is about 3000. BFP-D is deuterated BFP as described under Materials and Methods.

investigate the properties of the blue variant (Y66H), which contains a substitution that chemically alters the makeup of the chromophore, and also contains the substitution Y145F for enhanced fluorescent quantum efficiency (Heim & Tsien, 1996).

The three-dimensional structure of this mutant has been determined at 2.1 Å resolution and the model refined. The model revealed no major surprises as the overall fold of the molecule is essentially identical to wild type, and consists of an unusual 11 stranded  $\beta$  barrel surrounding the central chromophore-containing helix. The chromophore is fully formed, indicating that the machinery for catalyzing the backbone cyclization of residues 65 and 67 is more or less independent of the nature of the side chain at residue 66. Thus, with some ingenuity, it may be possible to substitute nonstandard amino acids at this locus in order to generate novel chromophores.

pH titrations of native BFP and chromopeptides derived from denatured, proteolytically degraded BFP indicate 3 charge states of the chromophore in aqueous solution, an acidic  $pK_a$  of 4.9 and a basic  $pK_a$  of 12.0, about 2 pH units lower than imidazole in solution due to extended conjugation. The absorption spectrum of the intact protein suggests that no significant fraction of the chromophore is ionized, and that the environment red-shifts the absorption spectrum substantially from that observed in aqueous solution. Fluorescence up-conversion spectroscopy revealed that the chromophore does not ionize in the excited state. It would be desirable to stabilize the anionic version of the chromophore to obtain a species that would emit at substantially longer wavelengths than the present emission maximum of 448 nm; re-engineering the hydrogen bond network around the chromophore may permit this to be achieved by substitution of groups that more closely match the basic  $pK_a$  of the chromophore.

The flexibility of the autocatalytic machinery for generating, and the ability of surrounding side chains to adjust the hydrogen bonding pattern to accommodate, non-native

chromophores is quite remarkable and bodes well for design and construction of useful GFP variants as tools for molecular and cell biologists.

## ACKNOWLEDGMENT

The fluorescence up-conversion experiments were carried out at the Stanford Free Electron Laser Center, supported by the Office of Naval Research. Partial support from the National Institutes of Health for acquisition of key components of the Ti:Sapphire laser is also gratefully acknowledged.

## REFERENCES

- Albert, A. (1968) in *Heterocyclic Chemistry*, p 441, Oxford University Press, New York.
- Brejč, K., Sixma, T. K., Kitts, P. A., Kain, S. R., Tsien, R. Y., Ormö, M., & Remington, S. J. (1997) *Proc. Natl. Acad. Sci. U.S.A.* (in press).
- Chalfie, M., Tu, Y., Euskirchen, G., Ward, W. W., & Prasher, D. C. (1994) *Science* 263, 802–805.
- Chatteraj, M., King, B. A., Bublitz, G. U., & Boxer, S. G. (1996) *Proc. Natl. Acad. Sci. U.S.A.*, 8362–8367.
- Cody, C. W., Prasher, D. C., Westler, W. M., Prendergast, F. G., & Ward, W. W. (1993) *Biochemistry* 32, 1212–1218.
- Cubitt, A. B., Heim, R., Adams, S. R., Boyd, A. E., Gross, L. A., & Tsien, R. Y. (1995) *Trends Biochem. Sci.* 20, 448–455.
- Gerdes, H.-H., & Kaether, C. (1996) *FEBS Lett.* 389, 44–47.
- Gryniewicz, G., Poenie, M., & Tsien, R. Y. (1985) *J. Biol. Chem.* 260, 3440–3448.
- Hamlin, R. (1985) *Methods Enzymol.* 114, 416–452.
- Heim, R., & Tsien, R. Y. (1996) *Curr. Biol.* 6, 178–182.
- Heim, R., Prasher, D. C., & Tsien, R. Y. (1994) *Proc. Natl. Acad. Sci. U.S.A.* 91, 12501–12504.
- Howard, A. J., Nielsen, C., & Xuong, N. H. (1985) *Methods Enzymol.* 114, 452–471.
- Jones, T. A. (1982) in *Computational Crystallography* (Sayre, D., Ed.) pp 303–317, Oxford University Press, Oxford, U.K.
- Jones, T. A., Zou, J.-Y., Cowan, S. W., & Kjeldgaard, M. (1991) *Acta Crystallogr., Sect. A* 47, 110.
- Lossau, H., Kummer, A., Heinecke, R., Pollinger-Dammer, F., Kompa, C., Bieser, G., Jonsson, T., Silva, C. M., Yang, M. M., Youvan, D. C., & Michel-Beyerle, M. E. (1996) *Chem. Phys.* 213, 1–16.
- Mitra, R. D., Silva, C. M., & Youvan, D. C. (1996) *Gene* 173, 13–17.
- Niwa, H., Inouye, S., Hirano, T., Matsuno, T., Kojima, S., Kubota, M., Ohashi, M., & Tsuji, F. I. (1996) *Proc. Natl. Acad. Sci. U.S.A.* 93, 13617–13622.
- Ormö, M., Cubitt, A. B., Kallio, K., Gross, L. A., Tsien, R. Y., & Remington, S. J. (1996) *Science* 273, 1392–1395.
- Palm, G. J., Zdanov, A., Gaitanaris, G. A., Stauber, R., Pavlakis, G. N., & Wlodawer, A. (1997) *Nat. Struct. Biol.* 4, 361–365.
- Prasher, D. C. (1995) *Trends Genet.* 11, 320–323.
- Rizzuto, R., Brini, M., De Giorgi, F., Rossi, R., Heim, R., Tsien, R. Y., & Pozzan, T. (1996) *Curr. Biol.* 6, 183–188.
- Stanley, R. J., & Boxer, S. G. (1995) *J. Phys. Chem.* 99, 859–863.
- Tronrud, D. E., Ten Eyck, L. F., & Matthews, B. W. (1987) *Acta Crystallogr., Sect. A* 43, 489–503.
- Ward, W. W., & Bokman, S. H. (1982) *Biochemistry* 21, 4535–4540.
- Ward, W. W., Cody, C. W., Hart, R. C., & Cormier, M. J. (1980) *Photochem. Photobiol.* 31, 611–614.
- Weast, R. C., Ed. (1974) in *CRC Handbook of Chemistry and Physics*, 55th ed., p D130, CRC Press, Cleveland, OH.
- Yang, F., Moss, L. G., & Phillips, G. N. (1996) *Nature Biotechnol.* 14, 1246–1251.

BI970563W